Proceedings of IMECE2002
ASME International Mechanical Engineering Congress & Exposition
November 17–22, 2002, New Orleans, Louisiana

IMECE2002-33632

BIFURCATION ANALYSIS FOR HORIZONTAL LONGITUDINAL FINS UNDER MULTI-BOILING CONDITIONS

Rizos N. Krikkis
Institute of Chemical Engineering and
High Temperature Chemical Processes.
P.O. Box 1414, Stadiou St., Platani
26500 Patras, Greece.

Stratis V. Sotirchos
Institute of Chemical Engineering and
High Temperature Chemical Processes.
P.O. Box 1414, Stadiou St., Platani
26500 Patras, Greece.

Panagiotis Razelos
Professor Emeritus, College of
Staten Island, CUNY, New York,
USA.

ABSTRACT

A numerical bifurcation analysis is carried out in order to determine the solution structure of a fin subject to multi-boiling heat transfer mode. The thermal analysis can no longer performed independently of the working fluid since the heat transfer coefficient is temperature dependent and includes the nucleate, the transition and the film boiling regime where the boiling curve is obtained experimentally for a specific fluid. The heat transfer process is modeled using one-dimensional heat conduction with or without heat transfer from the fin tip. Furthermore, five fin profiles are considered: the constant thickness, the trapezoidal, the triangular, the convex parabolic and the parabolic. The multiplicity structure is obtained in order to determine the different types of bifurcation diagrams, which describe the dependence of a state variable of the system (for instance the fin temperature or the heat dissipation) on a design (CCP) or operation parameter (base TD). Specifically the effects of the base TD, of CCP and of the Biot number are analyzed and presented in several diagrams since it is important to know the behavioral features of the heat rejection mechanism such as the number of the possible steady states and the influence of a change in one or more operating variables to these states. Stability analysis is carried out using the "resonance integral" technique and the Sturm-liouville eigensystem analysis.

INTRODUCTION

The study of extended surfaces operating under multi-boiling conditions has actually begun with the pioneer work of Westwater and co-workers [1-4]. The authors pointed out that the methods of fin design, so far developed, could not be used for the boiling case because the heat transfer coefficient was assumed uniform over the fin surface. Indeed if we assume for instance that the working fluid is water, the fin base TD is maintained at $\Delta T_b = 100^\circ\mathrm{C}$ and the fin tip TD is, say $\Delta T_e = 18.1^\circ\mathrm{C}$ then the ratio of the tip to base heat transfer coefficients can be obtained from Figure 1 as:

$$\frac{h_e}{h_b} = \frac{h(18.1^\circ\mathrm{C})}{h(100^\circ\mathrm{C})} = \frac{30116}{301} \approx 100$$

From the above argument it is evident the boiling heat transfer coefficient is highly non-uniform so that a different approach to the problem had to be taken. The authors therefore determined experimentally the heat transfer coefficient and used successfully a one-dimensional model including the effects of radiation for the prediction of the extended surfaces heat duty. Moreover, using the methodology of Wilkins [5], they obtained the optimum profile for longitudinal and pin fins under multi-boiling conditions. Haley and Westwater [2] concluded that the TD at the base of fin is not limited to the TD corresponding to the peak of the boiling curve, as it would have been in the absence of the fin. Actually it can be safely extended well above the critical value. From the design point of view an important result was that both boiling modes namely nucleate and transition are stable on a fin and can be utilized as a very efficient mechanism of heat transfer augmentation. Similar theoretical as well as experimental investigations were carried out at the Institute for High Temperatures of the Russian Academy of Sciences by Petukhov, Kovalev and co-workers [6-11]. Of particular interest is the work of Kovalev and

Rybchinskaya [10] who examined the simultaneous effects of multi-boiling and internal heat generation on the performance of a cylindrical pin fin. Specifically when both the aforementioned heat transfer mechanisms are present, for a given base heat flux the existence of four different base TD values are possible (see Figure 1 in [10]). The stability analysis was performed with the help of Liapunov's functional for two different types of boundary conditions.

Since the prediction of the heat duty under multi-boiling conditions is attractive many analytical solutions for simple (constant thickness) profiles can be found in the literature. Lai and Hsu [12] proposed a simple model for the determination of the length of the nucleate boiling section on a longitudinal fin of rectangular profile and the base heat dissipation of the fin. The authors divided the fin in several sections and each section was subjected to a different boiling mode. A global temperature and heat flux distribution was obtained by requiring that the temperature and its derivative at the base of one segment to match the corresponding values at the tip of the next segment. The same approach was adopted by Unal, [13], [14] in order to obtain closed form solutions for simple profile configurations. Liaw and Yeh [15], [16] conducted, in part I of their work, both a theoretical and an experimental investigation for a constant thickness profile longitudinal and pin fin with a heat transfer coefficient of the form of Eq.(1) for negative and positive exponents. The analytical solution was expressed in terms of the hypergeometric function. Both cases with and without heat transfer from the tip were examined. In addition they carried out a linear stability analysis for the transition boiling mode and its unstable nature was revealed from the resulting negative eigenvalues. In part II the authors considered multi-boiling heat transfer conditions for the same fins and used the previous obtained analytical solution and the methodology of Lai and Hsu [12] in order to determine the temperature distribution through the fin, which compared well with the experimental data for water and isopropyl alcohol. Recently Lee and co-workers [17-20], conducted a linear stability analysis for pin fins under two and three mode boiling using polynomial as well as trigonometric basis eigenfunctions. Their analysis was extended to include radial and longitudinal fins while the theoretical results were supported by experiments.

Bifurcation phenomena are common in chemical reaction engineering and a multitude of mathematical tools has been used for its investigation Aris [21]. The singularity theory, Golubitsky and Schaeffer [22], provides an efficient tool for the bifurcation analysis of physical systems described by a single algebraic equation and has been successfully employed by Balakotaih and Luss [23], [24] in the investigation of the multiplicity of a number of lumped-parameter systems and by Witmer *et al*. [25] in the investigation of a distributed diffusion and reaction problem. The two-point BVP of conduction-convection in a fin under multi-boiling conditions is similar to the reaction-diffusion BVP encountered in chemical engineering and the solution methodologies proposed by Michelsen and Villadsen, [26], Kubíček and Hlaváček [27], [28], Hsuen and Sotirchos [29], are generally applicable to the problem at hand. A complete picture of the bifurcation structure of the conduction-convection multi mode boiling system is still lacking, although many investigators have considered the fundamental mechanisms. This is because knowledge of the singular points of a system of equations provides local information about its multiplicity, but, by constructing the complete loci of the limit and hysteresis points of the solution diagram, global information may be obtained as well.

NOMENCLATURE

a_j	= boiling constants, Eq.(1)
A	= surface area, [m^2/m]
A_j	= dimensional constants, Eqs.(1), [W/(m^{2}K)]
Bi	= $(h_{\text{ref}} w/k)$ Biot number
B_L	= dimensionless parameter, Eq.(17)
D	= function defined by Eq.(23)
H	= fin length, [m]
k	= fin thermal conductivity, [W/(mK)]
L	= fin height, [m]
N_r	= removal number
O	= order of magnitude
P	= perimetry, [m/m]
q_f	= fin heat loss per unit length, [W/m]
Q	= dimensionless fin heat dissipation
Q_r	= reduced fin heat flux
S	= arc length, [m]
T	= temperature, [K]
X	= distance along fin, [m]
x	= (X/L) dimensionless distance along fin
Y	= fin semi-thickness, [m]
u	= conduction-convection coefficient
w	= fin semi-thickness, [m]

Greek Symbols

ΔT	= $(T - T_\infty)$ temperature difference, [K]
Θ	= $[(T - T_\infty)/(T_{\text{ref}} - T_\infty)]$ dimensionless fin temperature
λ	= (w_e/w_b) tip to base fin semi-thickness ratio
μ	= eigenvalue

Subscripts

b	= fin base
e	= fin tip
f	= fin, film boiling regime
n	= nucleate boiling regime
r	= reduced value (i.e. $h_r = h/h_{\text{ref}}$)
ref	= reference value
t	= transition boiling regime
TP	= turning point
∞	= ambient boiling liquid

Superscripts

$(\,')$	= derivative with respect to x
l	= lower steady state
u	= upper steady state

Abbreviations

BVP = Boundary Value Problem
CCP = Conduction-Convection Parameter
CP = Cusp Point
LAI = Length of Arc Idealization
ODE = Ordinary Differential Equation
TD = Temperature Difference
TP = Turning Point(s)

THE HEAT TRANSFER COEFFICIENT

A power-law function is usually used to express the heat transfer coefficient for the three boiling regimes , [2], [14]:

$$h_j = A_j (T - T_\infty)^{a_j}, \quad j = 1,2,3 \tag{1}$$

The TD at the knots for the nucleate-transition and for the transition-film section are calculated respectively as:

$$\ln \Delta T_{j+1-j} = \frac{\ln(A_j / A_{j+1})}{a_{j+1} - a_j}, \quad j = 1,2\,. \tag{2}$$

The boiling heat transfer coefficient for water together with the knot TD is depicted in Figure 1.

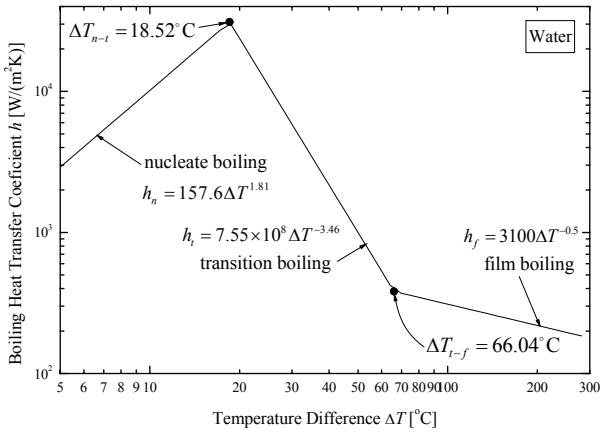

Figure 1. The boiling heat transfer coefficient of water.

The Chebychev Rational Model

Many algorithms for the numerical solution of ODE are based on the Taylor expansion and require continuity of the derivatives up to a high order. The previous equations have discontinuous derivatives at the knot TD and may produce unreliable results in the neighborhood close to the knot TD. In addition the sharp transition from one boiling section to the other is not experimentally observed, Haley and Westwater [2], Dhir and Liaw [33], an alternative relation has been developed for the representation of the boiling heat transfer coefficient of the following rational form:

$$\log h = \frac{\sum_{i=1}^{N_P} P_i z^{i-1}}{\sum_{i=1}^{N_Q} Q_i z^{i-1}}, \quad z = \log \Delta T \tag{3}$$

The resulting curve maintains the accurate representation of the experimental data and at the same time the sharp knot edges are smoothed. The required coefficients can be found in Tables 1 to 3.

P	i	Q
2.42204803823	1	1.00000000000
-1.56587017961	2	-1.32345998422
-1.37983071652	3	0.455402044288
1.26899698789	4	
-0.218079478341	5	

Table 1. Coefficients for the boiling heat transfer coefficient of water in Eq.(3).

P	i	Q
6.81696183207	1	1.00000000000
-19.1195164015	2	-1.04657133790
24.9191387614	3	0.363573429884
-15.6856514881	4	
4.67525093909	5	
-0.519507897020	6	

Table 2. Coefficients for the boiling heat transfer coefficient of isopropyl alcohol in Eq.(3).

P	i	Q
0.231661790336	1	1.00000000000
4.46761924528	2	-1.28376857095
-8.33566908328	3	0.418691192095
5.40219806954	4	
-1.49291322113	5	
0.159068566872	6	

Table 3. Coefficients for the boiling heat transfer coefficient of R-113 in Eq.(3).

STATEMENT OF THE PROBLEM

Consider a uniform density longitudinal fin depicted schematically in Figure 2 with symmetric profile $Y = Y(X)$ and thermal conductivity k. The fin has length H base thickness $2w$, tip thickness $2w_e$ and height L. The base of the fin is maintained at constant temperature T_b with the surrounding liquid at boiling temperature T_∞. The analysis is based on the following modified Murray [34] and Gardner [35] assumptions:

1. One-dimensional heat conduction.
2. The temperature at the fin base is uniform.
3. There are no heat sources or sinks in the fin.
4. The length of the fin H is much larger than either w or L.
5. The temperature of the boiling liquid is uniform.
6. The heat transfer coefficient h depends upon the local temperature difference ΔT ('local assumption'), Haley and Westwater [1].

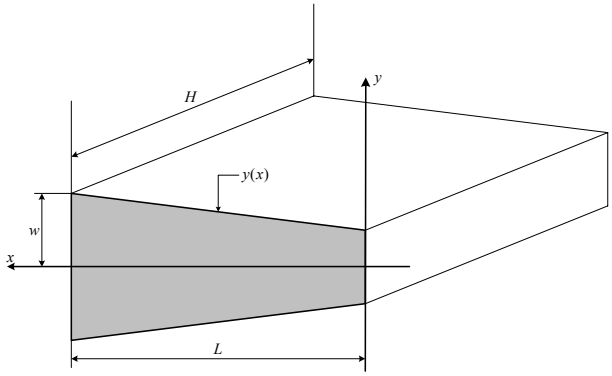

Figure 2. Longitudinal fin geometry.

On the basis of the above assumptions the conservation of energy yields the following differential equation that must be satisfied by the fin temperature:

$$\frac{d}{dX}\left(kA\frac{d\Delta T}{dX}\right)=P\frac{dS}{dX}h\Delta T \tag{4}$$

subject to the boundary conditions

$$\Delta T(L)=\Delta T_b \tag{5}$$

$$k(d\Delta T/dX)\big|_{X=0}=h_e\Delta T_e \tag{6}$$

at the fin base and fin tip respectively. In Eq.(4), $\Delta T=T-T_\infty$, $A=2Y(X)H$ is the area perpendicular to the heat flow and $P\approx 2H$ is the fin perimeter. The perimetry factor $P\,dS/dX$ is equal to

$$P\,dS/dX=2H\left[1+(dY/dX)^2\right]^{1/2} \tag{7}$$

Note that according to the earlier stated assumptions regarding the length of the fin, we can take $H=1\,\text{m}$ without loss of generality and all quantities will be per unit length. All the above equations are nondimensionalized with the aid of the following dimensionless variables:

$$x=X/L,\quad y=Y/w,\quad \Theta=(T-T_\infty)/(T_{\text{ref}}-T_\infty) \tag{8a,b,c}$$

Furthermore, the dimensionless parameters that describe the problem is the Conduction- Convection Parameter (CCP),

$$u^2=h_{\text{ref}}L^2/(kw)=L^2\text{Bi}/w^2 \tag{9}$$

and the Biot number,

$$\text{Bi}=h_{\text{ref}}w/k \tag{10}$$

where $h_{\text{ref}}=h(\Delta T_{\text{ref}})$ denotes the heat transfer coefficient at a reference temperature difference ΔT_{ref}. With the aid of Eq.(8b) the perimetry factor Eq.(7) may be written as:

$$P\frac{dS}{dX}=2\left[1+\frac{w^2}{L^2}\left(\frac{dy}{dx}\right)^2\right]^{1/2} \tag{11}$$

Using now the earlier defined Biot number and the CCP yields:

$$P\frac{dS}{dX}=2\left[1+\frac{\text{Bi}}{u^2}\left(\frac{dy}{dx}\right)^2\right]^{1/2} \tag{12}$$

On the basis of the previously stated assumption regarding the one dimensional heat conduction into the fin, the order of magnitude of the CCP is one and $\text{Bi}^{1/2}\ll 1$, Razelos and Georgiou [36]. Taking this into consideration Eq.(12) reduces to $P\,dS/dX\approx 2$. Substituting Eq.(8) into Eqs.(4) to (6) we obtain the following expression:

$$d^2\Theta/dx^2=(u^2h_r\Theta-y'\Theta')/y,\quad 0\le x\le 1 \tag{13}$$

where

$$h_r=h(\Theta\Delta T_{\text{ref}})/h_{\text{ref}} \tag{14}$$

is the reduced heat transfer coefficient while Θ'' and Θ' represent the second and the first derivatives with respect to x. The corresponding boundary conditions are

$$\Theta(1)=\Theta_b \tag{15}$$

$$\Theta'(0)=B_L\Theta(0)=B_L\Theta_e \tag{16}$$

where B_L is a dimensionless parameter:

$$B_L=h_eL/k=(h_e/h_{\text{ref}})u\text{Bi}^{1/2} \tag{17}$$

Using the same arguments as before Eq.(16) reduces to

$$\Theta'(0)\approx 0\,. \tag{18}$$

since $B_L\ll 1$. This is because u is of $O(1)$, $\Theta(0)$ is of $O(1)$ and $\text{Bi}^{1/2}\ll 1$. The equation that describes the profile of the fin is

$$y(x)=Y/w=\lambda+(1-\lambda)x^n \tag{19}$$

where $\lambda=1$ and $n=0$ corresponds to the rectangular profile.

Profile	λ	n
Rectangular	1.00	0
Trapezoidal	0.50	1
Triangular	0.05	1
convex parabolic	0.05	3/2
Parabolic	0.05	2

Table 4. Taper ratio and exponents for the profiles considered.

The values of the taper ratio λ and the profile exponent n considered in the present study are summarized in Table 4. It can be seen from Eq.(13) that the dimensionless temperature Θ and its derivative Θ' have the form:

$$\Theta=\Theta(x;u,\text{Bi},\Theta_b),\quad \Theta'=\Theta'(x;u,\text{Bi},\Theta_b) \tag{20a,b}$$

The heat dissipated by the fin,

$$q_f=kA\frac{dT}{dX}\bigg|_{X=L} \tag{21}$$

after introducing dimensionless variables becomes

$$Q = \frac{q_f}{2k\Delta T_{\text{ref}}} = \frac{w}{L}\Theta'(1) = \frac{\text{Bi}^{1/2}\Theta'(1)}{u} = \text{Bi}^{1/2} D \qquad (22)$$

where the heat flux parameter D is defined as:

$$D = \Theta'(1)/u \qquad (23)$$

It has been pointed out, Razelos and Georgiou [36], that the condition that will economically justify the use of fins is: "the ratio of heat dissipated by the fin to be much larger in comparison with the heat that would have been dissipated from the surface $2wH$, in the absence of the fin". This ratio is the removal number and it is equal to

$$N_r = \frac{q_f}{q_b} = \frac{2k\Delta T_{\text{ref}} Q}{(2w)h_b \Delta T_b} = \frac{D}{\text{Bi}^{1/2}}\left(\frac{h_{\text{ref}}/h_b}{\Theta_b}\right) \qquad (24)$$

Of particular interest is the fin reduced heat flux in terms of the critical heat flux as a measure of the fin performance:

$$Q_r = \frac{q_f/A_b}{q_{\text{CHF}}} = \frac{q_f/(2w)}{q_{\text{CHF}}} = \left(\frac{q_{\text{ref}}}{q_{\text{CHF}}}\right)\text{Bi}^{-1/2} D \qquad (25)$$

where $q_{\text{ref}} = h_{\text{ref}}\Delta T_{\text{ref}}$.

RESULTS AND DISCUSSION

The mathematical model presented in the previous sections is used here to study the multiplicity characteristics of a longitudinal fin under multi-boiling heat transfer mode. Because of the dependency of the boiling heat transfer coefficient on the TD, Eq.(13) is non-linear and multiple steady states exist at certain operating conditions. With multiple steady states we mean more than one temperature distributions for the fin that satisfy Eq.(13). This is clearly demonstrated in Figure 3 where for a given base TD ΔT_b there exist three different tip TD ΔT_e for $u > 0.2$ for example. In Figure 3 the tip TD is plotted against the base TD with water as the boiling liquid for a rectangular profile fin with an insulated tip. At each axes the corresponding knot TD ΔT_{n-t} and ΔT_{t-f} are also plotted and the corresponding boiling regimes (that is nucleate, transition and film) are also indicated. In this way a grid is generated which defines the boiling modes on the $(\Delta T_e, \Delta T_b)$ plane. Thus for a given base TD we can immediately identify the operating regime(s) of the base and the tip of the fin. From Eqs.(20) it is evident that the temperature distribution of the fin depends on the following parameters: the CCP, the Biot number and the dimensionless base TD Θ_b. For the construction of the $\Delta T_e - \Delta T_b$ diagram a working fluid, a fin profile and a reference TD are being selected while the CCP is kept constant and the BVP described by Eq.(13) is solved repeatedly for each value of the CCP. Hence a family of curves similar to those depicted in Figure 3 is obtained where u is the free parameter. A closer examination of Figure 3 reveals the following boiling modes:

- Single-mode boiling when $\Delta T_b < \Delta T_{n-t}$.
- Two-mode boiling when $\Delta T_{n-t} < \Delta T_b < \Delta T_{t-f}$ and $\Delta T_e < \Delta T_{n-t}$ that is transition and nucleate (TN) or when $\Delta T_{t-f} < \Delta T_b$ and $\Delta T_{n-t} < \Delta T_e < \Delta T_{t-f}$ that is film and transition (FT).
- Three-mode boiling (FTN) when $\Delta T_{t-f} < \Delta T_b$ and ΔT_e takes values in the three boiling regimes.

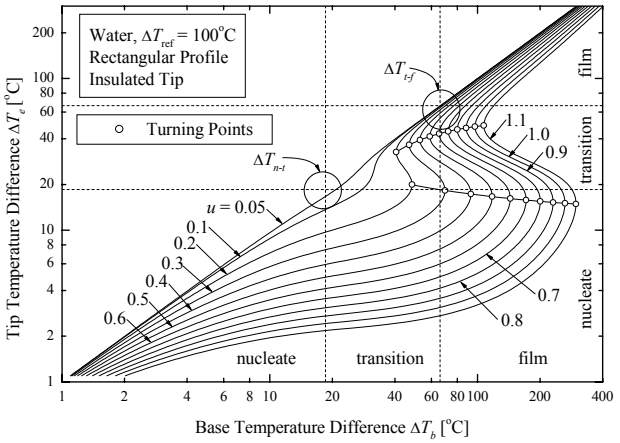

Figure 3. Loci of the turning points on the $(\Delta T_e, \Delta T_b)$ plane with the CCP as a parameter.

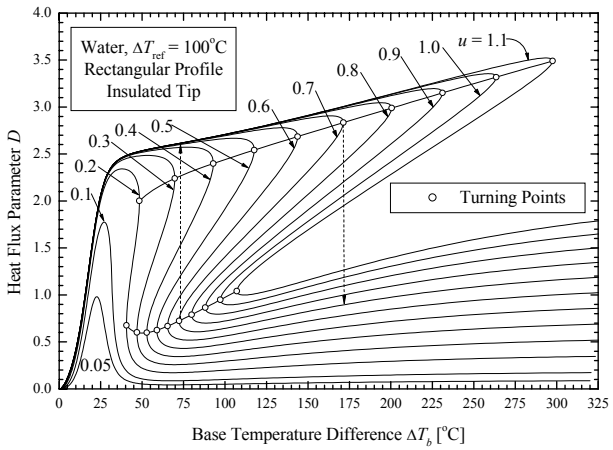

Figure 4. Hysteresis curves for the rectangular profile with insulated tip.

Another expected result is that as $\text{Bi} \to 0$, $u \to 0$, which means that $k \to \infty$ and the tip TD asymptotically equals the base TD: $\Delta T_e \simeq \Delta T_b$. For the further discussion of the bifurcation characteristics of the multi-boiling heat transfer mode the Turning Points (TP) [37-39], on the $\Delta T_e - \Delta T_b$ diagram will be introduced.

Bifurcation Diagrams and Temperature Distributions

On the TP change of the stability characteristics of the system is taking place and on the $(\Delta T_e, \Delta T_b)$ plane these TP are determined from the relation:

$$\partial \Delta T_b / \partial \Delta T_e = 0 \qquad (26)$$

and they are denoted with a characteristic symbol in Figure 3. Generally two TP exist in each curve with $u = \text{const.}$, the upper and the lower respectively. The upper TP $(\Delta T_e)^u_{\text{TP}}, (\Delta T_b)^u_{\text{TP}}$ corresponds to the upper steady state temperature distribution while the lower TP $(\Delta T_e)^l_{\text{TP}}, (\Delta T_b)^l_{\text{TP}}$ corresponds to the lower steady state temperature distribution (see Figure 6). For example for $u > 2$ there exist two TP while for $u < 2$ no TP exist since the base TD is a single value function of the tip TD and for that cases the fin can operate only on single-mode boiling. The TP define the values of the base TD for which multiple steady states exist. That is only when the condition

$$(\Delta T_e)^u_{\text{TP}} < \Delta T_b < (\Delta T_b)^l_{\text{TP}} \qquad (27)$$

is satisfied more than one (in fact three) temperature distributions exist. Moreover the TP separate the $\Delta T_e - \Delta T_b$ curves into the following three branches:

- Upper steady state branch: $\Delta T_e > (\Delta T_e)^u_{\text{TP}}$.
- Unstable steady state branch: $(\Delta T_e)^l_{\text{TP}} < \Delta T_e < (\Delta T_e)^u_{\text{TP}}$.
- Lower steady state branch: $\Delta T_e < (\Delta T_e)^l_{\text{TP}}$.

For example when the fin base operates at the transition regime, that is $\Delta T_{n-t} < \Delta T_b < \Delta T_{t-f}$ (i.e. two-mode boiling) there exist three operating points: one on the lower stable branch for which the tip TD corresponds to nucleate boiling, one on the unstable branch for which the tip TD corresponds to the transition boiling and one on the upper stable branch with the tip TD corresponding on the transition boiling. Therefore for two-mode boiling although two operating points are on the same boiling regime (i.e. transition) only one of them is stable. Furthermore when the fin base operates at the film regime, that is $\Delta T_{t-f} < \Delta T_b$ (i.e. three-mode boiling) there exist three operating points: one on the lower stable branch for which the tip TD corresponds to nucleate boiling, one on the unstable branch for which the tip TD corresponds to the transition boiling and one on the upper stable branch with the tip TD corresponding on the film boiling. Therefore the TP are the limiting stable operating points. Hence with the aid of Figure 3 we can recognize the mode of heat transfer mechanism (single-boiling or multi-boiling), the multiplicity pattern (one solution or three solutions) and the stability characteristics of each solution (stable or unstable).

Figure 4 represents the hysteresis curves. These are the curves of the dimensionless base heat dissipation as a function of the base TD with the CCP as the free parameter, which correspond to the same states of Figure 3. It is interesting to notice that in general there exist three base TD for a given value of the heat flux parameter and for a given *D* there exist three base TD values as it was first observed by Haley and Westwater [2]. Since the unsteady states are not realizable by the system the system it then expected at TP the state variables of the system (*D* and ΔT_b) to move to another stable operating point rather than trace the unstable branch. This behavior is indicated in Figure 4 for the curve with $u = 0.7$ and for a rectangular profile with insulated tip. During say a heating run when the upper TP is reached that is $\Delta T_b = (\Delta T_b)^u_{\text{TP}}$ then the system state variables will move in the direction of the arrow of the dashed line which connects the upper TP with the lower stable branch. A similar behavior is expected during a cooling run. When the lower TP is reached, $\Delta T_b = (\Delta T_b)^l_{\text{TP}}$ the state variables will move from the lower stable branch to the upper stable branch in the direction indicated by arrow of the dashed line, which connects the two branches.

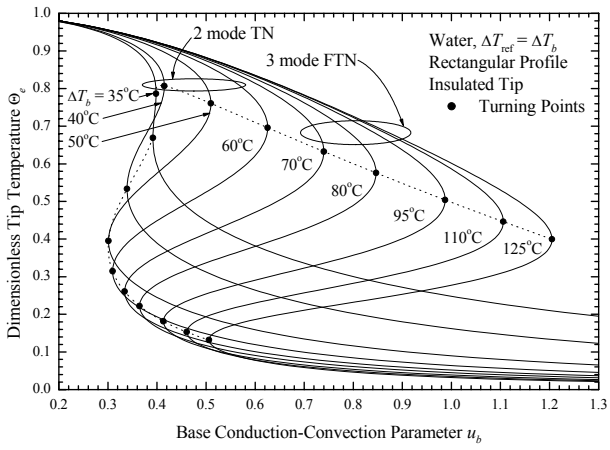

Figure 5. Loci of the turning points on the (Θ_e, u_b) plane for the rectangular profile with parameter the base temperature difference ΔT_b.

In the bifurcations diagrams of Figure 5 a family of sigmoid curves are shown for a rectangular profile with an insulated tip with the corresponding TP in each curve of constant base TD. It is observed that the CCP is a triple value function of the dimensionless tip TD in Figure 5. For the construction of these graphs a different parameterization of the problem has been selected. A value for ΔT_b is selected (i.e. from 35ºC to 125ºC) and the corresponding pair of variables (Θ_e, u_b) is obtained from the solution of Eq.(13). The TP are calculated from the relation

$$\partial u_b / \partial \Theta_e = 0 \qquad (28)$$

It should be noted here that the following relationship holds between *u* and u_b

$$u / u_b = (h_{\text{ref}} / h_b)^{1/2} \qquad (29)$$

In addition a dotted continuous line that connects the upper and the lower TP is plotted in Figure 5.

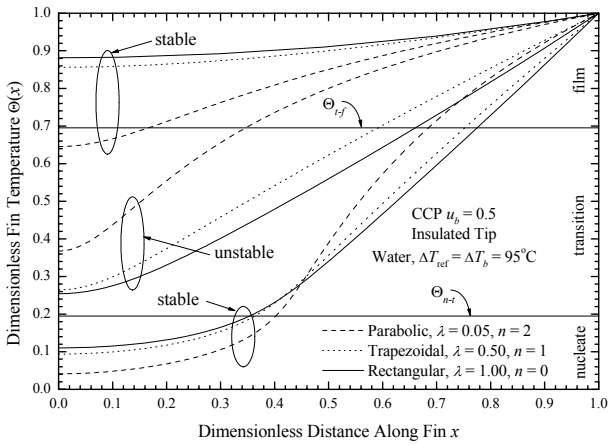

Figure 6. Stable and unstable temperature distributions for the rectangular, the trapezoidal and the parabolic profile.

	μ_i from Sturm-Liouville		
i	Upper SS	Unstable SS	Lower SS
1	-2.59	24.58	-6.57
2	-22.34	-15.24	-41.02
3	-61.81	-54.06	-65.23
4	-121.03	-112.60	-136.08
5	-199.99	-190.91	-208.08
6	-298.68	-289.24	-308.94
7	-417.12	-407.54	-427.09
8	-555.29	-545.67	-564.37

Table 5. Eigenvalues μ_i for the temperature profiles of Figure 6 from the Sturm-Liouville.

Local Stability Analysis

The existence of three (two stable and one unstable) temperature distributions $\Theta(x)$ along the fin height is demonstrated in Figure 6 for three different profiles. The rectangular ($\lambda = 1, n = 0$), the trapezoidal ($\lambda = 0.5$, $n = 1$) and the parabolic profile ($\lambda = 0.05$, $n = 2$) for the value of the CCP $u_b = 0.5$. The two dimensionless knot temperatures the nucleate-transition $\Theta_{n-t} = \Delta T_{n-t} / \Delta T_b = 0.1949$ and the transition-film $\Theta_{t-f} = \Delta T_{t-f} / \Delta T_b = 0.6952$ are also plotted as horizontal lines. The upper steady state temperature distributions for the rectangular and the trapezoidal profile show that the fin is operating under single-mode boiling, both the base and the tip TD are in the film regime. For the parabolic profile however is operation is being under two-mode boiling (FT) since the tip TD just enters the transition regime. For all the profiles the unsteady states are under two-mode boiling (FT), while the lower one is under three-mode boiling (FTN). The stability of a certain steady state $\Theta_{ss}(x)$ to small perturbations i.e. $\Theta = \Theta_{ss} + \vartheta$ is determined by the eigenvalues of the corresponding Sturm-Liouville problem (with insulated tip for simplicity) Wei [30], Luss and Lee [31], Aris [32], Michelsen and Villadsen [26]:

$$\frac{d}{dx}\left[y(x)\frac{d\vartheta}{dx} \right] - \left[u^2 \frac{\partial q_r(x)}{\partial \Theta} + \mu \right] \vartheta = 0 \qquad (30)$$

with

$$\vartheta'(0) = \vartheta(1) = 0, \quad 0 \le x \le 1$$

where $q_r = h_r \Theta$. All eigenvalues $\mu_1 > \mu_2 > \ldots > \mu_n > \ldots$ of the Sturm-Liouville problem, Eq.(30), are real and distinct and for $n \to \infty$, $\mu_n \to -(n\pi)^2$ but a finite number may be positive in which case $\Theta_{ss}(x)$ is an unsteady steady state. This is exactly the case for the unsteady state of Figure 6 where the eigenvalues of each steady state are given in Table 5 and in Table 6. The positive eigenvalue $\mu_1 = 24.6$ is the cause of the unstable character of the specific temperature distribution. For comparison purposes the eigenvalues for the rectangular profile have been computed with Wei's [30], "resonance integral" for a 30×30 matrix using the QR algorithm.

	μ_i from "resonance integrals"		
i	Upper SS	Unstable SS	Lower SS
1	-2.6	24.6	-6.6
2	-22.3	-15.2	-41.0
3	-61.8	-54.1	-65.2
4	-121.0	-112.6	-136.1
5	-200.0	-190.9	-208.1
6	-298.7	-289.2	-308.9
7	-417.1	-407.5	-427.1
8	-555.3	-545.7	-564.4

Table 6. Eigenvalues μ_i for the temperature profiles of Figure 6 from the "resonance integral" technique.

The locus of the TP on the (p_i, p_j) plane, where p_i and p_j are two of the model parameters divides the plane into two regions with different number of solutions. Figure 7 presents loci of TP on the $(u_b, \Delta T_b)$ plane for the rectangular profile with an insulated tip. It is seen that its locus of TP divides the $(u_b, \Delta T_b)$ plane into regions, one where a unique (type A) solution exists and another with three (type B) solutions. The number of solutions in each region is noted in Figure 7 inside a frame while the each solution locus together with the multiplicity pattern are given in the inserted graphs inside Figure 7. Its locus of TP exhibits a cusp point (CP), which is also indicated in Figure 7 and it is calculated from the following relations:

$$\partial u_b / \partial \Theta_e = \partial^2 u_b / \partial^2 \Theta_e = 0 \qquad (31)$$

As the base TD increases the CCP increases (except a small region of the lower branch between 35ºC and 50ºC), while the multiplicity region increases in size.

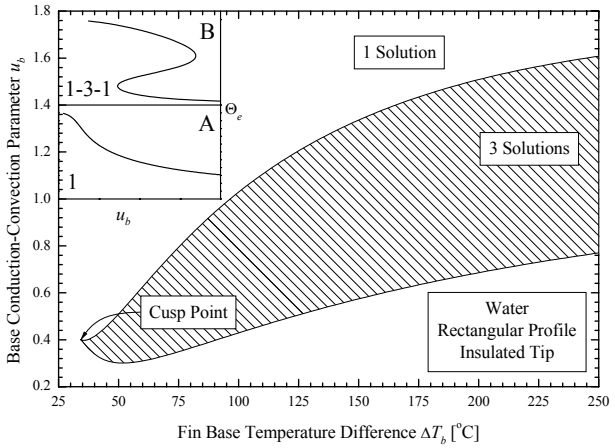

Figure 7. Loci of the turning points on the $(u_b, \Delta T_b)$ plane for the rectangular profile.

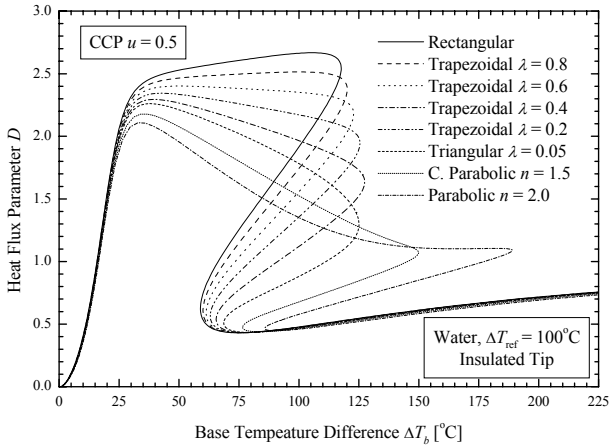

Figure 8. The effect of the profile on the hysteresis curves.

The Effect of the Profile on the Bifurcation Diagrams

Figure 8 shows the effect of the profile on the hysteresis curves. As the taper ratio λ decreases from 1(0.2)0.2 for the trapezoidal profiles, the TP move to higher base TD. Now as the taper ratio remains constant $(\lambda = 0.05)$ for the triangular, the convex parabolic and the parabolic profile and the profile exponent *n* increases from 1(0.5)2 the same trend is observed but much more intensive. Specifically the base TD increases by 10ºC for the triangular (comparing with the rectangular one), by 30ºC for the convex parabolic and by 70ºC for the parabolic. This is clearly indicated in Figure 8. Figure 8 reveals another worth noticing effect of the profile on the fin heat dissipation. From Figure 4 it is inferred that the maximum fin heat dissipation is quite close to the upper TP for the rectangular profile (about 120ºC for $u_b = 0.5$ in Figure 8). As the taper ratio decreases the corresponding base TD moves back to 30º-35ºC and the maximum heat flux decreases about 10% on the average for all the profiles. This is a shift of about 100ºC on the operating base TD, which is taking place for a relatively slight change of the profile taper (from rectangular $\lambda = 1$ to trapezoidal $\lambda \cong 0.7$).

In Figure 9 the effect of the profile on the multiplicity size is presented. A significant reduction is observed as a result of the corresponding reduction on the CCP TP for the various profiles. Additionally the CP CCP decreases and the CP base TD remains almost unchanged.

The Effect of the Biot Number on the Bifurcation Diagrams

The effect of the Biot number will be considered only for the rectangular profile since for the other profiles the heat transfer are at the tip is significantly decreased and the heat transfer from the tip is unimportant. As the Biot number increases the multiplicity region decreases as it is presented in Figure 10. Figure 11 shows the remarkable effect of the Biot number on the hysteresis curves. Comparing with the insulated tip case the upper TP has increased by 80ºC while the maximum heat dissipation is increased by 20% approximately. For the lower TP however only an increase of about 10ºC is observed in the base TD TP while the increase in the heat dissipation is of the order of 5%. In addition as the Biot number increases the curve on the upper TP becomes sharper.

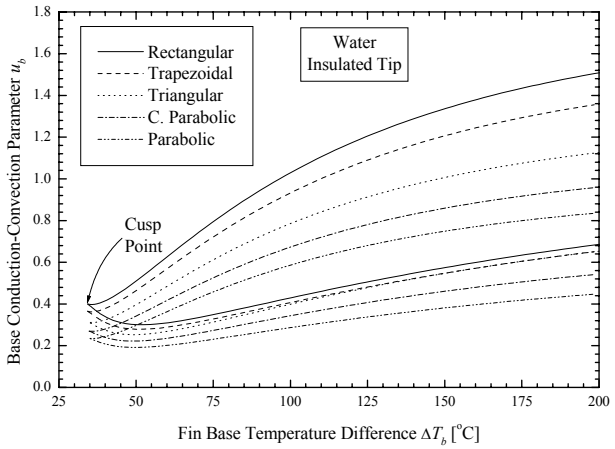

Figure 9. Loci of the turning points on the $(u_b, \Delta T_b)$ plane for the five profiles.

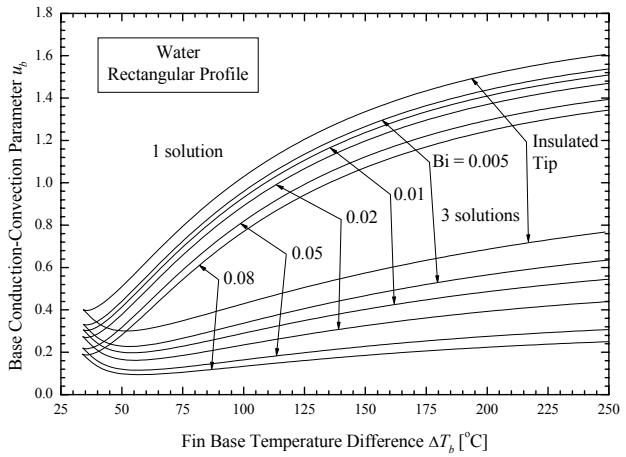

Figure 10. The effect of Biot number on the locus of the turning points on the $(u_b, \Delta T_b)$ plane for the rectangular profile.

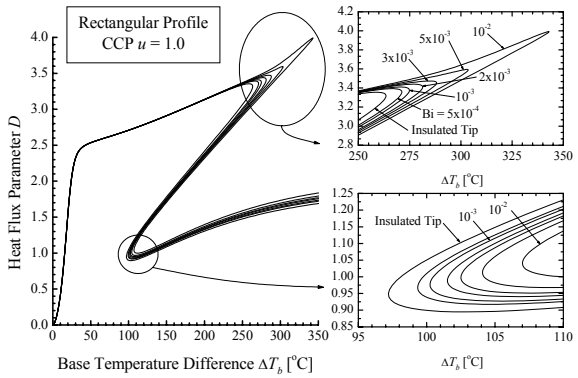

Figure 11. The effect of the Biot number on the hysteresis curves for the rectangular profile.

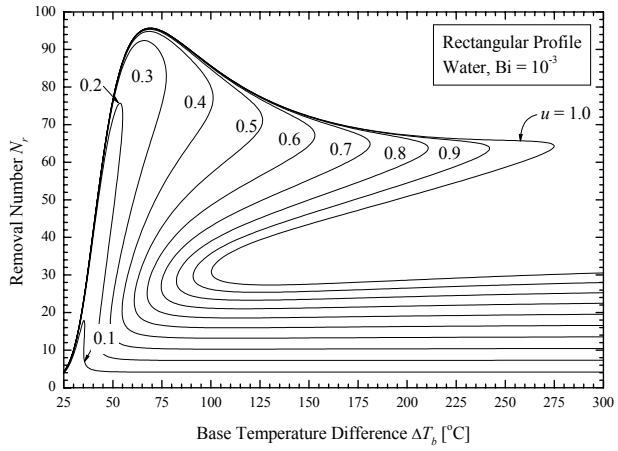

Figure 12. The removal number N_r as a function of the base TD and the CCP for the rectangular profile fin.

Fin Performance and Comparison with Experimental Data

Figure 12 shows the removal number for the rectangular profile fin where values as high as 100 can be reached. At the same time the dimensionless heat flux in terms of the critical heat flux in Figure 13 is of the order of 6. This clearly demonstrates that the use of an extended surface under multi-boiling conditions constitutes a powerful heat transfer enhancement mechanism. In Figure 14 and in Figure 15 a comparison between the calculated and the experimental data of Liaw and Yeh [16] are presented since for the rectangular profile fin and the corresponding cylindrical pin fin the governing equations are identical. For isopropyl alcohol the calculations are in reasonable agreement for the upper branch while for the lower branch the film boiling data should be modified since these values are obtained from extrapolation. Similar results were given by Haley and Westwater [2] for the case of isopropyl alcohol. For water the agreement is generally better except of the area of the upper TP where an "overshooting" is predicted. It is suspected that this is because of the sharp peak near the nucleate-transition neighborhood (although the smoother rational curve was used) in conjunction with the high value of the transition-boiling exponent b. Numerical experiments with smoother boiling curves show that the radius of curvature at the ΔT_{n-t} knot is increased the calculated curves complies with the experimental data.

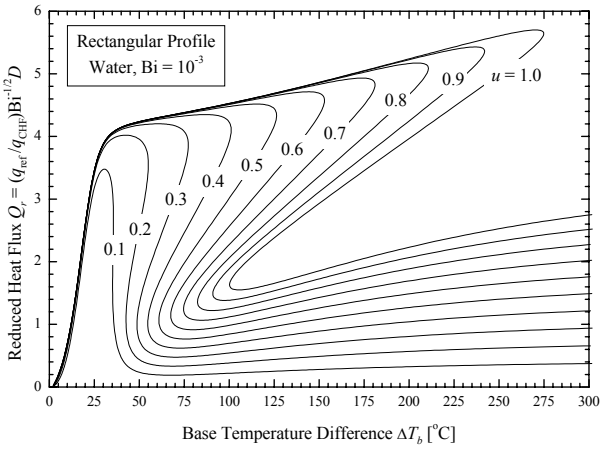

Figure 13. The reduced heat flux Q_r of the base TD and the CCP for the rectangular profile fin.

CONCLUSIONS

In the present study a numerical bifurcation analysis has been carried out for longitudinal fin under multi-boiling heat transfer mode. Five profiles were considered: the rectangular, the trapezoidal, the triangular, the convex parabolic and the parabolic one. The theoretical model is based on the one dimensional heat conduction with and without heat transfer from the tip while a rational function of the TD were used to correlate the boiling heat transfer coefficient. Important conclusions are:

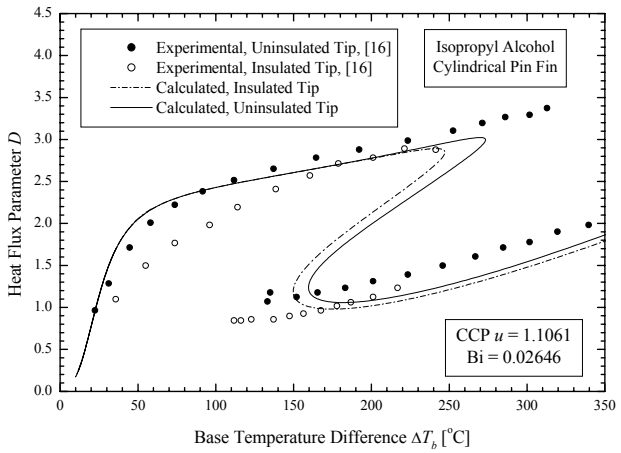

Figure 14. Comparison of the calculated and measured heat flux data for isopropyl alcohol for a cylindrical pin fin.

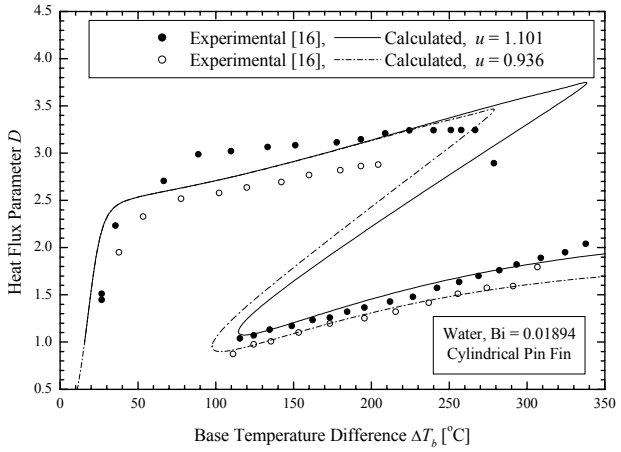

Figure 15. Comparison of the calculated and measured heat flux data for water for a cylindrical pin fin.

I. The base TD ΔT_b, the CCP u and the Biot number Bi are the important operating variables of the boiling system under consideration.
II. The taper ratio λ and the profile exponent n have a profound effect on the fin heat dissipation and on the size of the multiplicity region.
III. The Biot number has an important effect on the stable operating range and on the maximum heat dissipation for a rectangular profile fin. Moreover, as the Biot number increases the multiplicity region increases.
IV. The use of an extended surface can be very beneficial since the removal number can take values up to 100 while the heat flux developed shows a six-fold increase.

REFERENCES

[1] Haley, K., W., and Westwater, J., W., (1965), "Heat transfer from a fin to a boiling liquid", *Chem Eng. Sci.*, vol. 20, pp. 711.

[2] Haley, K., W., and Westwater, J., W., (1966), "Boiling heat transfer from single fins", *Proc. 3rd International Heat Transfer Conference*, AIChE-ASME, Vol. 3, pp. 245-253.

[3] Klein, G., J., and Westwater, J., W., (1973), "Heat Transfer from Multiple Spines to boiling liquids", *AIChE Journal*, Vol. 17, no. 5, pp. 1050-1056.

[4] Shih, C-C, and Westwater, J., W., (1974), "Spheres, hemispheres and discs as high-performance fins for boiling heat transfer", *Int. J. Heat Mass Transfer*, vol. 17, pp. 125-133.

[5] Wilkins, J., E., Jr., (1960), "Minimum Mass Thin Fins for Space Radiators", *Proc. Heat Transfer and Fluid Mechanics Institute*, 228, Stanford university Press.

[6] Petukhov, B., S., Kovalev, S., A., Zhukov, V., M., and Kazakov, G., M., (1971), "Measurment of local heat transfer on a nonisothermal surface", *High Temp.*, vol. 9, no 6. pp. 1159-1161.

[7] Petukhov, B., S., Kovalev, S., A., and Zhukov, V., M., (1973), "Local boiling heat transfer on nonisothermal surfaces", *Heat Transfer Sov. Res.*, vol. 5, no 6, pp. 154-162.

[8] Kovalev, S., A., (1964), "Stability of the boiling regimes", *Teplofiz. Vys. Temp.* vol. 2, no. 5, pp. 780-789 (in Russian).

[9] Kovalev, S., A., (1966), "An investigation of minimum heat fluxes in pool boiling of water", *Int. J. Heat Mass Transfer*, vol. 9, pp. 1219-1226.

[10] Kovalev, S., A., and Rybchinskaya, G., B., (1978), "Prediction of the stability of pool boiling heat transfer to finite disturbances", *Int. J. Heat Mass Transfer*, vol. 21, pp. 694-700.

[11] Kovalev, S., A., Zhukov, V., M., and Usatikov, S., V., (2000), Comment on the paper by Lin, W., W., Yang, J., C., and Lee, D., J., (2000), "Metastable pin fin boiling", *Int. J. Heat Mass Transfer*, vol. 43, no. 9, pp. 1629-1635, *Int. J. Heat Mass Transfer*, vol. 44, no. 18, pp. 3575-3577.

[12] Lai, F-S., and Hsu, Y-Y., 1967, "Temperature Distribution in a Fin Partially Cooled by Nucleate Boiling", *AIChE Journal*, vol. 13, no. 4, pp. 817-821.

[13] Unal, H., C., (1985), "Determination of the temperature distribution in an extended surface with a non-uniform heat transfer coefficient", *Int. J. Heat Mass Transfer*, vol. 28, no. 12, pp. 2279-2284.

[14] Unal, H., C., (1987), "An analytic study of boiling heat transfer from a fin", *Int. J. Heat Mass Transfer*, vol. 30, no. 2, pp. 341-349.

[15] Liaw, S., P., and Yeh, R., H., (1994), "Fins with temperature dependent surface heat flux-I. Single heat transfer mode", *Int. J. Heat Mass Transfer*, vol. 37, no. 10, pp. 1509-1515.

[16] Liaw, S., P., and Yeh, R., H., (1994), "Fins with temperature dependent surface heat flux-II. Multi-boiling heat transfer", *Int. J. Heat Mass Transfer*, vol. 37, no. 10, pp. 1517-1524.

[17] Lin, W., W., and Lee, D., J., (1996), "Boiling on a Straight Pin Fin", *AIChE Journal*, vol. 42, no. 10, pp. 2721-2728.

[18] Lin, W., W., and Lee, D., J., (1998), "Boiling on a plate fin and annular fin *Int. Comm. Heat Mass Transfer*, vol. 25, no. 8, pp.1169-1180.

[19] Lin, W., W., Yang, J., C., and Lee, D., J., (1999), "Boiling on a conical spine", *Experimental Heat Ttransfer*, vol. 12, pp. 175-191.

[20] Lin, W., W., Yang, J., C., and Lee, D., J., (2000), "Metastable pin fin boiling", *Int. J. Heat Mass Transfer*, vol. 43, no. 9, pp. 1629-1635.

[21] Aris, R., (1975), *The Mathematical Theory of Diffusion and Reaction in Permeable Catalysts*, Vols. 1 and 2, Clarendon Press, Oxford.

[22] Golubitsky, M., and Scaeffer, D., (1985), *Singularities and Groups in Bifurcation Theory*, Vol. 1 and 2, Springer, New York.

[23] Balakotaiah, V., and Luss, D., (1982), "Structure of the steady state solutions of lumped-parameter chemically reacting systems", *Chem. Engng. Sci.*, Vol. 37, pp. 1611-1623.

[24] Balakotaiah, V., and Luss, D., (1982), "Global analysis of the multiplicity features of multi-reaction lumped multi-parameter systems", *Chem. Engng. Sci.*, Vol. 39, pp. 865-881.

[25] Witmer, G., Balakotaiah, V., and Luss, D., (1986), "Finding singular points of two-point boundary value problems", *J. Comp. Phys.*, Vol. 65, pp. 244-250.

[26] Michelsen, M., L., and Villadsen, J., (1972), "Diffusion and reaction on spherical catalysts: steady state and local stability analysis", *Chem. Engng. Sci.*, Vol. 27, pp. 751-762.

[27] Kubíček, M., and Hlaváček, V., (1971), "Solution of non-linear boundary value problems-III. A novel method: differentiation with respect to an actual parameter", *Chem. Engng. Sci.*, Vol. 26, pp. 705-709.

[28] Kubíček, M., and Hlaváček, V., (1974), "Solution of non-linear boundary value problems-VIII. Evaluation of branching points based on shooting method and GPM technique", *Chem. Engng. Sci.*, Vol. 29, pp. 1695-1699.

[29] Hsuen, H., K., D., and Sotirchos, S., V., (1989), "Multiplicity analysis of intraparticle char combustion", *Chem. Engng. Sci.*, Vol. 44, no 11, pp. 2639-2651.

[30] Wei, J., (1965), "The stability of a reaction with intra-particle diffusion of mass and heat: The Liapunov methods in a metric function space", *Chem. Engng. Sci.*, Vol. 20, pp. 729-736.

[31] Luss, D., and Lee, J., C., M., (1968), "On global stability in distributed parameter", *Chem. Engng. Sci.*, Vol. 23, pp. 1237-1248.

[32] Aris, R., (1969), "On stability criteria of chemical reaction engineering", *Chem. Engng. Sci.*, Vol. 24, pp. 149-169.

[33] Dhir, V., K., and Liaw, S., P., (1989), "Framework for a Unified Model for Nucleate and Transition Pool Boiling", *ASME. J. Heat Transfer*, vol. 111, pp. 739-746.

[34] Murray, M., W., (1938), "Heat transfer through an annular disk or fin of uniform thickness", *ASME Journal of Applied Mechanics*, vol. 60A, pp. 278.

[35] Gardner, K., A., (1945), "Efficiency of extended surfaces", *Trans. ASME*, vol. 69 no. 8, pp. 621-631.

[36] Razelos, P., and Georgiou, E., (1992), "Two-Dimensional Effects and Design Criteria for Convective Extended Surfaces", *Heat Transfer Engineering*, Vol. 13, no. 3, pp. 38-48.

[37] Seydel R., (1994), *Practical Bifurcation and Stability Analysis. From Equilibrium to Chaos*, Springer-Verlag, New York.

[38] Govaerts, W., J., F., (2000), *Numerical Methods for Bifurcations of Dynamical Equilibria*, SIAM, Philadelphia.

[39] Iooss, G., and Joseph, D., D., (1990), *Elementary Stability and Bifurcation Theory*, 2nd ed., Springer-Verlag, New York.